
How Much is Left? LLMs Linearly Encode Their Remaining Output Length

Mohamed Amine Merzouk^{1,2} Dmitri Carpov³ Mirko Bronzi³ Damiano Fornasiero³
Adam Oberman^{2,3}

¹Mila, Quebec AI Institute ²McGill University ³LawZero

Abstract

Large language models generate one token at a time, yet their responses show remarkably consistent length structure: step-by-step solutions converge in predictable token counts, retrievals stop after a few sentences, retractions extend responses by measurable amounts. We ask whether the model carries an internal estimate of how much response remains. Training minimal-capacity linear probes on frozen hidden states of three open-weight 7-8B models across seven completion-style datasets, we find three converging pieces of evidence. First, total response length is linearly decodable from the prompt’s last hidden state alone, before any output is emitted. Second, probe directions trained on natural-language datasets transfer broadly, including to controlled synthetic completions never seen in training, outperforming a statistical baseline; the converse direction generally fails, and this asymmetry is itself informative. Third, on curated high-loss completions, the probe’s per-position estimate shifts upward at the moment the model retracts and restarts a partial solution, a directional behavior no position-only predictor can reproduce (we note in §4.3 that this is qualitative, not aggregate). We frame this as approximate estimation of remaining generation length, distinct from exact-counting impossibility results for transformers, and interpret it as evidence that LLMs maintain a plan-like internal representation of output length (decodable, not necessarily used causally).

Code: <https://anonymous.4open.science/r/llm-output-length>

1 Introduction

When a large language model produces a step-by-step solution, retrieves a fact, or writes a paragraph, the result has a length: a number of tokens emitted before an end-of-sequence (EOS) token. That length is often surprisingly predictable from the prompt alone. Asked to solve a grade-school arithmetic problem, current LLMs tend to produce three-to-five lines of working before the answer; asked to retrieve a date, they produce a single short clause. This consistency is at odds with the standard description of how an autoregressive model computes: each token is sampled conditioned on the prefix, with no explicit notion of total response length anywhere in the computation graph.

This paper asks whether that consistency is an artifact of decoding (token-by-token sampling that happens to terminate at similar lengths) or whether the model’s intermediate representations *encode* an estimate of how much response remains. The distinction matters: in the first case, length is a downstream statistical regularity of the conditional distribution; in the second, the model carries an internal variable for “remaining work,” informally a *plan*. Recent mechanistic work shows that LLMs plan ahead over *content*, e.g., committing to a rhyme word several positions before writing the line that ends in it [Lindsey et al., 2025]; we ask the analogous question for *length*.

We attack this question with linear probing [Alain and Bengio, 2018, Belinkov, 2021]. For a frozen LLM and a (prompt, completion) pair (x, y) with completion length T , we extract the residual-stream hidden states h_t at every position t and train minimal-capacity linear probes to predict the remaining

token count $r_t = T - t$. The use of a linear probe is deliberate: any signal we recover is information that is *already linearly available* in the hidden state, not a result of the probe’s own computation. We compare against a constant statistical baseline (the train-split median of r_t , the optimal constant predictor under L^1 loss) and against a length-minus-position predictor seeded with the model’s own prompt-end estimate of total length, so that any improvement of the per-position probe is attributable to mid-completion residuals rather than to position alone.

Two methodological caveats motivate the rest of our design. First, we are *estimating* remaining generation length, not exactly counting items in the input: our headline numbers are on the order of MAE ≈ 30 tokens on a 400-token completion, a useful low-precision signal that is unrelated to the exact-counting impossibility theorems for transformers [Yehudai et al., 2026] (see §2 for the distinction). Second, linear probes for LLM internals are typically evaluated only within distribution; we additionally report cross-dataset matrices for every (model, source dataset, target dataset) triple to test how much of the recovered signal is a property of the model’s representation versus a fit to a single dataset’s marginal.

A third, qualitative observation complements these results: because the Remaining Count Probe predicts from h_t rather than t , it is not constrained to be monotonic, and on curated high-MAE completions \hat{r}_t shifts upward at the retraction token (“Wait, let me try again”; Figure 3). We present this as directional only — absolute predictions on this example are far from r_t , and a length-matched non-retraction control would license the stronger “plan-update” reading (§4.3 and Limitations).

A reliable readout of the model’s own length estimate has practical applications: a retraction token without an upward shift in \hat{r}_t is a candidate signature of unfaithful chain-of-thought, and a prompt-end estimate \hat{T}_0 exceeding a budget is a cheap early-termination signal. We do not pursue either here, but both motivate the probing study that follows.

Contributions.

1. We define a small probe family — a Remaining Count Probe, a constant-median statistical baseline, and a Completion Length Probe with exact countdown — that stratifies the residual stream’s contribution into within-prompt decodability and mid-completion update.
2. Out-of-distribution evaluation: a probe trained on a *natural-language* corpus beats the constant-median predictor on most natural-language and synthetic targets, including ones it never saw; probes trained on the synthetic Count/Countdown sets transfer within that pair but fail on natural-language targets (Tables 3–10). The asymmetry suggests natural-language training recovers a more general length-tracking direction.
3. Qualitative dynamic re-estimation: a curated retraction example (Figure 3) and high-MAE gallery (Appendix A.9) isolate a class of directional updates no position-only predictor can produce. The aggregate version is flagged as future work.

2 Related Work

Linear probes for LLM internals, and OOD generalization. Training a small linear probe on frozen activations to predict a property of interest goes back to Alain and Bengio [2018], with subsequent work showing that linguistic structure [Tenney et al., 2019, Hewitt and Manning, 2019], latent beliefs about truth [Burns et al., 2024, Marks and Tegmark, 2024], world-model state [Li et al., 2024, Nanda et al., 2023], and safety-relevant behaviour [Arditi et al., 2024, Zou et al., 2025] are linearly recoverable from intermediate representations; theoretical accounts of the *linear representation hypothesis* [Elhage et al., 2022, Park et al., 2024] explain when this should be expected. Belinkov [2021] cautions that probe accuracy reflects what is decodable, not what the model functionally uses. OOD evaluations of LLM probes are scarce and transfer is often weak (a notable exception is the cross-lingual refusal direction [Arditi et al., 2024]); evaluation is especially sparse for continuous regression targets on residual streams like our r_t . Our cross-dataset matrices (§5) close that gap.

Planning, aha moments, and dynamic re-estimation. Whether LLMs “plan” is a recently active question. Lindsey et al. [2025] use circuit tracing to show that Claude commits to a rhyme word before writing the line that ends in it, planning over *content*; we ask the analogous question over

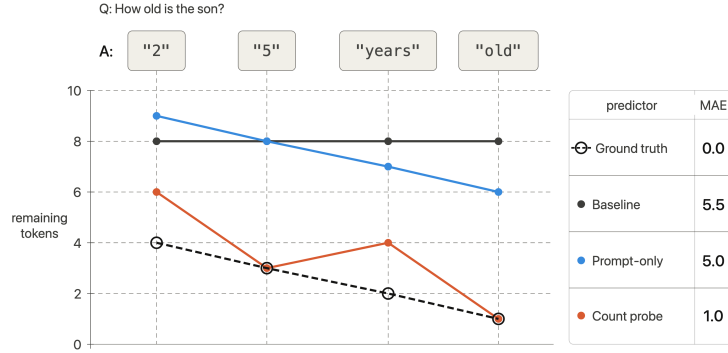


Figure 1: Predicting remaining tokens on a short example. The answer to “How old is the son?” has ground truth remaining counts 4, 3, 2, 1 (dashed line, hollow markers). The constant baseline outputs the dataset median at every position. The prompt-only probe is trained on the prompt’s final hidden state and decremented by one at each step, capturing the right shape but with a systematic offset (9→8→7→6). The Remaining Count Probe reads the residual stream at every position; its predictions (6→3→4→1) are non-monotonic, yet it achieves the lowest MAE (1.0 vs. 5.0 and 5.5). Section 4 and Figure 3 show a real example with the retraction-token spike.

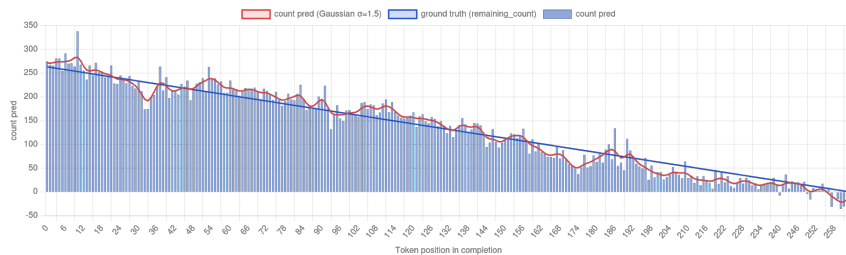
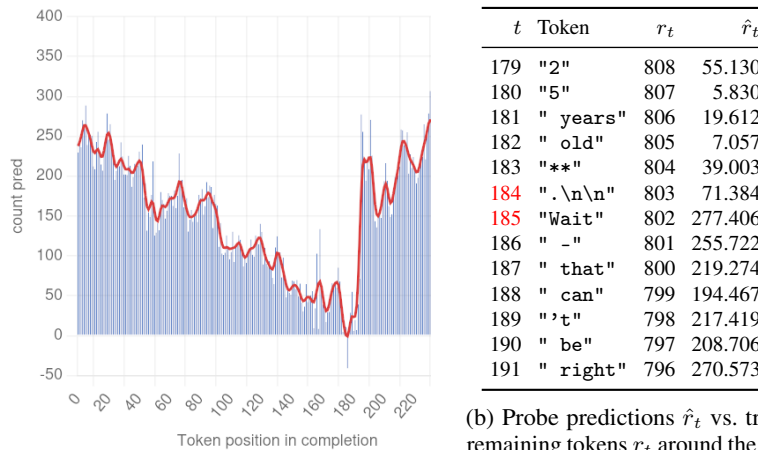


Figure 2: Count prediction versus ground truth on a typical example with small MAE.



(a) Count prediction on a high-MAE example, zoomed in around the retraction.

(b) Probe predictions \hat{r}_t vs. true remaining tokens r_t around the retraction (red: ".\n\n", "Wait").

Figure 3: A high-MAE retraction example, drawn from the worst-MAE region of the eval set (selection as in §A.9). See discussion in §4.3.

length. Mid-trace shifts around the DeepSeek-R1 “aha moment” [Guo et al., 2025] have been read both sceptically [d’Aliberti and Ribeiro, 2026, Liu et al., 2025, Huang et al., 2024] and mechanistically [Yang et al., 2025, Zhao et al., 2026, Boppana et al., 2026]; closest in method is Boppana

et al. [2026], whose linear probe reads out answer-confidence at every reasoning step. Our retraction-shift observation has the same shape but on the length variable. Engineered counterparts such as s1 [Muennighoff et al., 2025] confirm that “Wait”-token interventions affect test-time compute.

Token counting in transformers (orthogonal to this work). A separate literature studies *exact in-context counting* in transformers: the $d \geq m$ phase transition of Yehudai et al. [2026], attention over-squashing on global aggregation [Barbero et al., 2024], and BPE boundary effects [Singh and Strouse, 2024]. Our target is different: a continuous regression on hidden states for the number of tokens the model itself will go on to produce (headline MAE ≈ 30 on a 400-token completion), not a 0/1 exact count over the prompt. The two threads are complementary; impossibility results for exact counting do not bear on approximate estimation of remaining generation length.

3 Methodology

3.1 Problem Formulation

Let M be a frozen autoregressive language model and let (x, y) denote a (prompt, completion) pair, where $y = (y_1, \dots, y_T)$ is generated by M until either an end-of-sequence token is emitted at position T or a maximum-length cutoff is reached. We say that (x, y) *terminates naturally* when an EOS token is emitted; only naturally terminated sequences are used for training and evaluation. For each completion position $t \in \{1, \dots, T\}$, we define the target:

$$r_t = T - t \quad (\text{remaining token count}), \quad (1)$$

The empirical question is whether $h_t^{(\ell)}$ contains enough information to predict r_t . The probe family of §3.3 answers it by comparing predictors with different access to h_t versus t , against two reference predictors that use no information from the residual stream during generation.

3.2 Hidden State Extraction

For each token position t in a (prompt, completion) sequence — including the prompt — we extract the residual-stream activation $h_t^{(\ell)} \in \mathbb{R}^d$ at every transformer layer $\ell \in \{0, \dots, L\}$, computed by a single forward pass over the *full* sequence with M ’s parameters frozen. Probes are trained on completion positions only; prompt positions contribute no loss except where explicitly stated for the Completion Length Probe (§3.3, item 3), whose loss is masked everywhere except at the prompt’s last position.

3.3 Probe Family

A probe $f_\theta : \mathbb{R}^d \rightarrow \mathbb{R}$ is a single linear layer with no nonlinearity. This minimal capacity is deliberate: strong probe performance reflects information that is already *linearly available* in $h_t^{(\ell)}$ rather than computation performed by the probe. We compare three predictors of the per-position remaining-count target $r_t = T - t$, illustrated for a four-token completion in Figure 1:

The **Remaining Count Probe** $f_\theta(h_t^{(\ell)}) \rightarrow \hat{r}_t$ regresses on the residual-stream activation at every completion position with loss $\mathcal{L}_{\text{count}} = (\hat{r}_t - r_t)^2$. Since the prediction depends on $h_t^{(\ell)}$ rather than t , this probe is not constrained to be monotonic in t , a freedom we exploit in §4.3.

The **statistical baseline** outputs $\hat{r}_t = \tilde{r}$, the median of r_t over the train split, at every position; it is the optimal constant predictor under L^1 loss and our natural reference for MAE (§3.4).

The **Completion Length Probe** is a regression probe trained only on the prompt’s last hidden state with target T ,

$$\mathcal{L}_{\text{prompt-only}} = (\hat{T} - T)^2 \quad \text{evaluated only at } t = \text{prompt_length} - 1, \quad (2)$$

masked elsewhere. At evaluation, the prompt-end prediction \hat{T}_0 is reused at every completion position via the deterministic exact countdown

$$\hat{r}_t = \max(\hat{T}_0 - t - 1, 0).$$

The countdown uses no information from h_t during generation; it shares the position structure of a length-minus-position baseline but substitutes the model’s own prompt-end estimate of T . Our headline number at the prompt-end position is $\text{prompt_AE} = |\hat{T}_0 - T|$ (§4.1).

All three regression predictors share a single LM forward pass per minibatch and a single dataloader, so any difference in evaluation performance is attributable to the per-probe target rather than to sampling variance.

A complementary family of K -way classification probes is reported as an ablation in Appendix A.8.

3.4 Statistical Baselines

The optimal constant predictor under L^1 loss is the median: for a real-valued X with median m , $\arg \min_c \mathbb{E}|X - c| = m$, in direct parallel with the mean as the squared-loss minimizer. Since every regression number we report is MAE, the natural reference is the constant-median predictor $\hat{r}_t = \tilde{r}$ (§3.3 item 2) fit on the train split. Its MAE on the train marginal is exactly the Mean Absolute Deviation about the median, the L^1 analogue of variance.

A probe with MAE below this floor is therefore extracting information about r_t beyond what any position-independent predictor can achieve from the train marginal alone.

3.5 Loss and Optimization

Let \mathcal{P} denote the set of active probes and let $\mathcal{L}_p(\theta_p; \text{batch})$ denote the per-probe loss. For each minibatch we (i) compute hidden states, (ii) for each $p \in \mathcal{P}$, compute \mathcal{L}_p , run the backward pass, and step the per-probe optimizer, and (iii) clear the per-probe gradients. The base model is never updated. Optimizer, learning rate, batch size, max steps, scheduler settings, and per-dataset configured split sizes are listed in Appendix A.4.

3.6 Evaluation

The headline metric for every regression result is per-token mean absolute error (MAE) — the natural counterpart to the constant-median statistical baseline introduced in §3.4. MAE aggregates cleanly over completions of varied length and bounds gracefully against the MAD-about-the-median floor without further normalization. We report MAE in two ways: as a token-weighted dataset-wide average (every completion-position contributes one term to the mean) and, when comparing the Completion Length Probe to its constant baseline, as the absolute error at the prompt-end position alone. Classification-probe metrics (accuracy and Cohen’s κ) are reported as a complementary ablation in Appendix A.8.

3.7 Models and Datasets

Models. We evaluate three open-weight instruction-tuned base models in the 7–8B parameter range: Llama-3.1-8B-Instruct [Grattafiori et al., 2024], Olmo-3-7B-Instruct [Groeneveld et al., 2024], and Mistral-7B-Instruct-v0.3 [Jiang et al., 2023]. The three families differ in tokenizer, pretraining mixture, and instruction-tuning recipe, which lets us check whether the length signal is a property of one model family or a more general feature of instruction-tuned LLMs.

We use seven completion-style datasets in total: two synthetic and five standard.

Synthetic (controlled-length) datasets. **Count** consists of completions to the prompt "Count from 0 to {n}. Only output the numbers separated by a space. Start now:", and **Countdown** of completions to "Count down from {n} to 0. Only output the numbers separated by a space. Start now:". In both cases $n \in [0, 300]$. These two sets give us a controlled regime in which the eventual completion length T is exactly determined by the prompt: a probe that performs well on Count and Countdown is verifiably reading the relevant information out of the residual stream and not relying on dataset-wide regularities.

Standard datasets. Covering reasoning, retrieval, and open-ended writing, we use **GSM8K** [Cobbe et al., 2021], (grade-school math), **MATH** [Hendrycks et al., 2021] (competition-level math), **MMLU-Pro** [Wang et al., 2024] (multiple-choice with reasoning rationales), **OpenThoughts-1k** [Guha et al.,

2025] (long-form reasoning traces), and **TriviaQA** [Joshi et al., 2017] (short-form retrieval). Together with Count and Countdown this yields seven datasets spanning a wide range of expected response lengths and structural regularities, a prerequisite for the cross-dataset experiments in §5. The system prompts and the source field of the user message for each dataset are listed in Appendix A.5.

We extract hidden states for both train and eval splits in a single forward pass per example, then re-use the cache for every probe in the family (§3.3) and the per-layer variants reported in Appendix A.1, so the computational cost of training the entire probe family is dominated by the one LM forward pass per example.

4 Results

All numbers in this section are the mean across three independent training seeds; per-seed variance was less than 1 token of MAE — well below the spread across (model, dataset) cells — so we omit per-seed error bars. Headline MAEs are token-weighted averages over the eval split; Appendix A.3 reports a per-completion-length breakdown.

4.1 Preliminary: Completion Length Probe results

Table 1 reports the prompt-end MAE of the Completion Length Probe (§3.3, item 3) versus the constant-median statistical baseline. The probe beats the baseline on every (model, dataset) cell. The improvement is largest on the synthetic Countdown set, where Llama’s prompt-end MAE drops to 5.27 tokens against a 150.18 baseline — T is a deterministic function of the prompt for these examples, and a linear readout recovers it almost exactly. On the natural-language sets the gap is smaller but consistent across all three model families: prompt-end MAE is roughly half to three-quarters of the constant baseline (Appendix A.2). The headline claim — total response length is linearly decodable from the prompt’s last hidden state alone, before any output is emitted — holds in every cell of the table.

Table 1: Prompt-end absolute error of the Completion Length Probe versus the constant-median statistical baseline. Each cell is the MAE in tokens between the predicted total completion length \hat{T}_0 and the realized T , evaluated only at the prompt’s last position and averaged across the eval split. Lower is better; bold marks the winner per (model, dataset). Mistral-7B / TriviaQA was omitted due to computational limitations.

Model	Count	Countdown	GSM8K	MATH	MMLU-Pro	OpenThoughts-1k	TriviaQA
Llama-3.1-8B							
Statistical baseline	150.17	150.18	58.66	166.32	204.21	212.24	57.86
Completion Length Probe	29.73	5.27	42.29	115.29	117.19	141.65	44.20
Olmo-3-7B							
Statistical baseline	147.67	150.58	116.17	194.05	204.82	272.58	160.56
Completion Length Probe	31.22	8.40	80.46	132.13	134.86	199.13	110.84
Mistral-7B							
Statistical baseline	263.15	265.12	84.81	174.71	196.16	195.77	–
Completion Length Probe	135.09	35.92	74.92	132.28	131.51	165.36	–

4.2 Probe vs. statistical baseline vs. Completion Length countdown

Table 2 compares the per-token MAE of the Remaining Count Probe against the constant-median statistical baseline and against the exact-countdown predictor (the Completion Length Probe’s prompt-end estimate \hat{T}_0 broadcast as $\max(\hat{T}_0 - t - 1, 0)$).

Implied claim. The three-way comparison in Table 2 stratifies the residual stream’s contribution. Exact countdown is a stronger baseline than it appears: it receives the position t as an explicit input through $\max(\hat{T}_0 - t - 1, 0)$, while the Remaining Count Probe sees only h_t and must recover any position-dependent component from it; in expectation Exact countdown’s per-token MAE is just $|\hat{T}_0 - T|$, the prompt-end probe’s accuracy. The breakdown is: (i) when the Remaining Count Probe

Table 2: Per-token MAE on each (model, dataset) cell, in tokens, token-weighted mean across the eval split (every completion-position contributes one term to the mean). The constant-median statistical baseline is the same constant at every position; the exact-countdown predictor uses the model’s prompt-end estimate \hat{T}_0 and decrements by one each step; the Remaining Count Probe reads h_t at every position. Lower is better; bold marks the winner per cell.

Model	Count	Countdown	GSM8K	MATH	MMLU-Pro	OpenThoughts-1k	TriviaQA
Llama-3.1-8B							
Statistical baseline	117.81	117.82	70.15	151.20	172.49	187.83	61.09
Exact countdown	29.80	4.82	44.04	123.32	123.31	129.09	60.94
Remaining Count Probe	34.41	4.38	36.59	109.87	123.56	131.47	50.05
Olmo-3-7B							
Statistical baseline	116.54	117.84	124.32	178.83	184.82	219.01	151.00
Exact countdown	31.59	8.64	94.51	131.87	127.19	191.75	140.88
Remaining Count Probe	33.36	4.50	76.65	123.10	133.54	195.97	116.75
Mistral-7B							
Statistical baseline	197.45	200.23	91.67	161.41	171.10	179.71	–
Exact countdown	137.77	37.36	82.90	132.19	141.05	158.16	–
Remaining Count Probe	69.51	20.81	66.94	122.23	138.55	133.63	–

beats the constant-median baseline, the residual stream encodes information about r_t beyond what any position-independent predictor can deliver from the train marginal alone; (ii) when it further beats Exact countdown, the residual stream at *mid-completion* positions adds information beyond what was already linearly readable at the prompt’s last position — the length estimate is updated during generation rather than committed at the prompt and decremented from there; (iii) when the two are within noise, the prompt-end estimate is sufficient and mid-completion positions add no additional linear information for r_t . Cells where the Remaining Count Probe ties or loses to Exact countdown are therefore the mechanical restatement of case (iii), not a contradiction. Appendix A.2 re-presents Tables 1 and 2 with each entry normalized by the constant-median baseline.

4.3 Dynamic re-estimation: the probe spikes when the model restarts

Because the Remaining Count Probe’s prediction at position t is a function of h_t rather than of t , it is *not constrained* to be monotonic. The constant-median baseline and the exact-countdown predictor are monotonically non-increasing by construction; any upward jump in the probe’s per-token prediction is therefore something neither reference predictor can reproduce. We do not aggregate this gap into a number across the eval set; rather, we use a single curated example to make the qualitative point that the per-position estimate *can* update in response to events inside the model’s own generation.

Phenomenology. The probe’s predictions track the ground truth closely on most completions (Figure 2), but on a small fraction MAE is much larger. Figure 3 shows one such case. The point of the panel is the *directional* change in \hat{r}_t : at the ".\n\n"/"Wait" pair (the model’s own retraction) the probe’s prediction shifts upward from 71 to 277, while the true r_t continues to decrement monotonically — an upward movement no monotonic-in- t baseline can produce. The probe’s *absolute* predictions on this completion are far from the truth throughout the window (e.g., 4.84 at $t = 173$ against a true $r_t = 814$), so what is interpretable is the sign of the per-position update at the retraction token, not the level. We read this as evidence that the residual stream may carry a *plan-like* representation that updates when the model recognizes it must redo work.

The within-distribution absolute-tracking behavior and the directional-update behavior are both present in the probe but on different completions; demonstrating them on the same example, and aggregating the directional update against a length-matched control, is flagged as future work in Limitations. We expect the aggregate version to recover the same directional pattern: the constant-median and exact-countdown baselines cannot produce upward $\Delta\hat{r}_t$ at *any* position by construction, while the probe does so at retraction tokens whenever we look. Appendix A.9 shows the same shift on four additional completions, triggered by different retraction phrases (“Wait”, “But let’s check”, “let’s look again”) at different absolute positions.

5 Cross-dataset generalization of the Remaining Count Probe

The cross-dataset matrix is not symmetric, and the asymmetry is the result. Probes trained on natural-language datasets generalize broadly, including back into the controlled synthetic regime; probes trained on the controlled synthetic sets do not generalize to natural language. The remainder of this section unpacks both halves and the regularization-style explanation we offer for the gap.

For each model, we trained a Remaining Count Probe on every available dataset and evaluated it on every other dataset. We present the Llama-3.1-8B-Instruct matrix in the main text (Table 3); the analogous Mistral-7B-Instruct-v0.3 and Olmo-3-7B-Instruct matrices are in the appendix (Tables 9 and 10). The Llama and Mistral matrices report the five datasets for which the full train×eval grid was available; the Olmo matrix reports all seven (see §3.7).

Table 3: Remaining Count Probe cross-token MAE (mean across 3 seeds) on Llama-3.1-8B. Rows: train dataset; columns: eval dataset. Each train-dataset row is followed by a *baseline* row giving the median-baseline MAE fit on that dataset’s train split, reported on five datasets.

Train	Count	Countdown	GSM8K	MMLU-Pro	OpenThoughts-1k
Count	35.07	99.17	101.21	228.93	280.02
<i>baseline</i>	117.81	117.82	87.12	176.54	208.25
Countdown	183.81	4.13	87.84	236.40	278.57
<i>baseline</i>	117.81	117.82	87.12	176.54	208.25
GSM8K	130.91	149.68	38.79	164.27	199.74
<i>baseline</i>	129.59	129.59	70.15	201.75	241.90
MMLU-Pro	105.01	118.96	63.57	121.51	147.25
<i>baseline</i>	118.83	118.84	98.93	172.68	201.28
OpenThoughts-1k	100.37	101.03	107.94	133.05	136.69
<i>baseline</i>	147.44	147.45	175.60	175.51	187.83

Reading the matrix. The headline pattern recurs across all three models: off-diagonal entries (probe trained on one dataset, evaluated on another) are often still below the eval dataset’s own baseline, showing that the probe direction trained on one corpus carries a non-trivial component of length information that survives the dataset shift.

The off-diagonal structure is strikingly asymmetric along a single axis: *synthetic vs. natural*. Probes trained on the synthetic Count and Countdown sets transfer poorly to natural-language datasets: on Llama-3.1-8B (Table 3) a Count-trained probe scores MAE 228.93 on MMLU-Pro against a 176.54 baseline; Mistral-7B and Olmo-3-7B reproduce the same picture (Tables 9 and 10). Within the synthetic pair the probes *do* transfer (Count → Countdown achieves 99.17 against a 117.82 baseline on Llama), consistent with the two tasks sharing a near-identical surface structure.

The natural-language datasets behave in the opposite direction. On Llama-3.1-8B, an OpenThoughts-1k-trained probe beats the eval-side baseline on *every* other dataset in its row, including the two synthetic ones; likewise for the MMLU-Pro-trained probe. Mistral-7B and Olmo-3-7B reproduce the same picture: the strongest transfer sources are the datasets with the longest and most heterogeneous completions (OpenThoughts-1k, MMLU-Pro, and to a lesser extent GSM8K), and probes trained on them generalize *back into* the synthetic regime despite never having seen it.

We read this as a regularization story. The synthetic sets pin T to a single deterministic feature of the prompt; a linear probe fit on them latches onto whichever direction in h_t correlates with that feature, and that direction does not coincide with the model’s general length-tracking direction. The natural-language sets, by contrast, force the probe onto a direction that explains length variation across many prompt structures — the same direction that also covers the trivial synthetic cases. The diagonal remains the best entry in every row, but the off-diagonal pattern is inconsistent with a probe that has only memorized its source dataset’s marginal distribution of T .

Tokenization differences are also unparsimonious as the load-bearing explanation: a tokens-per-character story predicts symmetric transfer failures, but the matrix shows one-way generalization (natural → synthetic, not the converse), and natural-language probes transfer broadly across GSM8K, MMLU-Pro, OpenThoughts-1k, and TriviaQA despite their heterogeneous tokenization profiles. A shared-BPE replication is left to follow-up work.

6 Limitations

Decodability does not entail causal use. Linear probes recover information that is *available* in the residual stream; they do not show that the model *uses* the identified direction during generation. The natural follow-up is an activation-patching study that ablates or steers the length-tracking direction at inference time and measures the effect on the realized output length. Until that experiment is run, every claim in this paper about a “plan” should be read as a claim about representation, not about mechanism.

The dynamic re-estimation evidence is qualitative, not aggregate. The five cases (one in §4.3, four more in Appendix A.9) are surfaced by sorting eval-set completions on per-completion MAE; they are qualitative, not an aggregate measurement. A second caveat compounds the first: these examples are drawn from the worst-MAE region of the eval set by construction, and on those completions the probe’s *absolute* predictions are far from the ground truth (single digits against $r_t \approx 800$ in Figure 3). The panels are therefore licensed to show only the *direction* of the per-position update, not its level. The within-distribution absolute-tracking result of §4.1–4.2 and the directional retraction-spike behavior of §4.3 are both present in the probe but on different subsets of the eval set, and we do not currently demonstrate them on the same example. The stronger “plan-update” reading would be licensed by (i) showing the upward shift is significantly larger at retraction tokens than at length-matched non-retraction controls in the same MAE regime, and (ii) recovering the same directional behavior on completions where the probe’s absolute predictions track r_t closely; both are tractable on the existing eval cache and are the immediate next step.

Model scale and training regime. All three evaluated models are 7–8B-parameter instruction-tuned checkpoints. We do not know whether the length-tracking direction sharpens, weakens, or relocates at frontier scale, or in base (non-instruction-tuned) models whose completion-length distribution differs structurally. Our per-layer sweep (Appendix A.1) is on one model only and should not be read as a claim about layer localization in the three headline models.

Reduced grid coverage. Compute limits forced two omissions: Mistral-7B / TriviaQA is dropped throughout, and the Llama and Mistral cross-dataset matrices cover five of the seven datasets rather than all seven (the Olmo matrix covers all seven).

Selection bias toward naturally-terminated sequences. Training and evaluation are restricted to completions that emit EOS before the max-length cutoff (§3.2); sequences that run to the cutoff are excluded by construction. Our results therefore speak to length estimation conditional on successful termination, not to the harder question of whether the model “knows” when its own generation is going to overrun.

7 Conclusion

We have shown that the residual stream of an LLM linearly encodes an internal estimate of how many tokens of its own response remain to be generated, and that this estimate has three properties consistent with a plan-like representation rather than a downstream regularity of decoding. (i) It is decodable from the prompt’s last hidden state alone: the model has committed to an approximate response length before emitting the first generated token. (ii) The probe direction recovered from natural-language datasets transfers across datasets with markedly different length distributions, weakening a pure memorize-the-marginal explanation; the converse direction (synthetic to natural) does not transfer, and §5 attributes the asymmetry to natural-language training forcing the probe onto a more general length-tracking direction. (iii) On curated examples the estimate can update directionally: at the moment the model retracts a partial solution and restarts, the probe’s prediction shifts upward, a behavior no position-only predictor can produce by construction.

Result (iii) is qualitative, not aggregate (§4.3 and Limitations); the natural follow-up is the aggregate retraction analysis we describe there. That analysis is also the most direct starting point for the safety and capabilities applications sketched in §1.

References

- Guillaume Alain and Yoshua Bengio. Understanding intermediate layers using linear classifier probes, 2018. URL <https://arxiv.org/abs/1610.01644>.
- Andy Arditi, Oscar Balcells Obeso, Aaqib Syed, Daniel Paleka, Nina Rimsky, Wes Gurnee, and Neel Nanda. Refusal in language models is mediated by a single direction. In *The Thirty-eighth Annual Conference on Neural Information Processing Systems*, 2024. URL <https://openreview.net/forum?id=pH3XAQME6c>.
- Federico Barbero, Andrea Banino, Steven Kapturowski, Dharshan Kumaran, João G. M. Araújo, Alex Vitvitskiy, Razvan Pascanu, and Petar Veličković. Transformers need glasses! information over-squashing in language tasks, 2024. URL <https://arxiv.org/abs/2406.04267>.
- Yonatan Belinkov. Probing classifiers: Promises, shortcomings, and advances, 2021. URL <https://arxiv.org/abs/2102.12452>.
- Siddharth Boppana, Annabel Ma, Max Loeffler, Raphael Sarfati, Eric Bigelow, Atticus Geiger, Owen Lewis, and Jack Merullo, 2026. URL <https://arxiv.org/abs/2603.05488>.
- Collin Burns, Haotian Ye, Dan Klein, and Jacob Steinhardt. Discovering latent knowledge in language models without supervision, 2024. URL <https://arxiv.org/abs/2212.03827>.
- Karl Cobbe, Vineet Kosaraju, Mohammad Bavarian, Mark Chen, Heewoo Jun, Lukasz Kaiser, Matthias Plappert, Jerry Tworek, Jacob Hilton, Reiichiro Nakano, Christopher Hesse, and John Schulman. Training verifiers to solve math word problems, 2021. URL <https://arxiv.org/abs/2110.14168>.
- Liv G. d’Aliberti and Manoel Horta Ribeiro. The illusion of insight in reasoning models, 2026. URL <https://arxiv.org/abs/2601.00514>.
- Nelson Elhage, Tristan Hume, Catherine Olsson, et al. Toy models of superposition, 2022. URL <https://arxiv.org/abs/2209.10652>.
- Aaron Grattafiori, Abhimanyu Dubey, Abhinav Jauhri, et al. The llama 3 herd of models, 2024. URL <https://arxiv.org/abs/2407.21783>.
- Dirk Groeneveld, Iz Beltagy, Pete Walsh, et al. Olmo: Accelerating the science of language models, 2024. URL <https://arxiv.org/abs/2402.00838>.
- Etash Guha, Ryan Marten, Sedrick Keh, et al. Openthoughts: Data recipes for reasoning models, 2025. URL <https://arxiv.org/abs/2506.04178>.
- Daya Guo, Dejian Yang, Haowei Zhang, et al. Deepseek-r1 incentivizes reasoning in llms through reinforcement learning. *Nature*, 645(8081), 2025. ISSN 1476-4687. doi: 10.1038/s41586-025-09422-z. URL <http://dx.doi.org/10.1038/s41586-025-09422-z>.
- Dan Hendrycks, Collin Burns, Saurav Kadavath, Akul Arora, Steven Basart, Eric Tang, Dawn Song, and Jacob Steinhardt. Measuring mathematical problem solving with the math dataset, 2021. URL <https://arxiv.org/abs/2103.03874>.
- John Hewitt and Christopher D. Manning. A structural probe for finding syntax in word representations. In *NAACL*, 2019. URL <https://aclanthology.org/N19-1419/>.
- Jie Huang, Xinyun Chen, Swaroop Mishra, Huaixiu Steven Zheng, Adams Wei Yu, Xinying Song, and Denny Zhou. Large language models cannot self-correct reasoning yet, 2024. URL <https://arxiv.org/abs/2310.01798>.
- Albert Q. Jiang, Alexandre Sablayrolles, Arthur Mensch, et al. Mistral 7b, 2023. URL <https://arxiv.org/abs/2310.06825>.
- Mandar Joshi, Eunsol Choi, Daniel S. Weld, and Luke Zettlemoyer. Triviaqa: A large scale distantly supervised challenge dataset for reading comprehension, 2017. URL <https://arxiv.org/abs/1705.03551>.

- Kenneth Li, Aspen K. Hopkins, David Bau, Fernanda Viégas, Hanspeter Pfister, and Martin Wattenberg. Emergent world representations: Exploring a sequence model trained on a synthetic task, 2024. URL <https://arxiv.org/abs/2210.13382>.
- Jack Lindsey, Wes Gurnee, Emmanuel Ameisen, et al. On the biology of a large language model, 2025. URL <https://transformer-circuits.pub/2025/attribution-graphs/biology.html>.
- Zichen Liu, Changyu Chen, Wenjun Li, Penghui Qi, Tianyu Pang, Chao Du, Wee Sun Lee, and Min Lin. Understanding r1-zero-like training: A critical perspective, 2025. URL <https://arxiv.org/abs/2503.20783>.
- Samuel Marks and Max Tegmark. The geometry of truth: Emergent linear structure in large language model representations of true/false datasets, 2024. URL <https://arxiv.org/abs/2310.06824>.
- Niklas Muennighoff, Zitong Yang, Weijia Shi, Xiang Lisa Li, Li Fei-Fei, Hannaneh Hajishirzi, Luke Zettlemoyer, Percy Liang, Emmanuel Candès, and Tatsunori Hashimoto. s1: Simple test-time scaling, 2025. URL <https://arxiv.org/abs/2501.19393>.
- Neel Nanda, Andrew Lee, and Martin Wattenberg. Emergent linear representations in world models of self-supervised sequence models, 2023. URL <https://arxiv.org/abs/2309.00941>.
- Kiho Park, Yo Joong Choe, and Victor Veitch. The linear representation hypothesis and the geometry of large language models, 2024. URL <https://arxiv.org/abs/2311.03658>.
- Aaditya K. Singh and DJ Strouse. Tokenization counts: the impact of tokenization on arithmetic in frontier llms, 2024. URL <https://arxiv.org/abs/2402.14903>.
- Ian Tenney, Dipanjan Das, and Ellie Pavlick. Bert rediscovers the classical nlp pipeline, 2019. URL <https://arxiv.org/abs/1905.05950>.
- Yubo Wang, Xueguang Ma, Ge Zhang, et al. Mmlu-pro: A more robust and challenging multi-task language understanding benchmark, 2024. URL <https://arxiv.org/abs/2406.01574>.
- Shu Yang, Junchao Wu, Xin Chen, Yunze Xiao, Xinyi Yang, Derek F. Wong, and Di Wang. Understanding aha moments: from external observations to internal mechanisms, 2025. URL <https://arxiv.org/abs/2504.02956>.
- Gilad Yehudai, Haim Kaplan, Guy Dar, Royi Rassin, Asma Ghandeharioun, Mor Geva, and Amir Globerson. When can transformers count to n ?, 2026. URL <https://arxiv.org/abs/2407.15160>.
- Jiachen Zhao, Yiyu Sun, Weiyan Shi, and Dawn Song. Can aha moments be fake? identifying true and decorative thinking steps in chain-of-thought, 2026. URL <https://arxiv.org/abs/2510.24941>.
- Andy Zou, Long Phan, Sarah Chen, et al. Representation engineering: A top-down approach to ai transparency, 2025. URL <https://arxiv.org/abs/2310.01405>.

A Additional Results

A.1 Per-layer probe sweep

To localize where in M the length signal is most accessible, we extend the probe family across layers: we train a separate Remaining Count Probe on the hidden state at each individual layer $\ell \in \{0, \dots, L\}$. Figure 4 reports MAE-vs-layer. MAE is significantly higher on early layers, decreases sharply through the middle of the network, and stabilizes in the upper third around 80.

Two takeaways follow. First, most of the length-tracking information is encoded in the late layers: the early layers’ predictions sit essentially at the constant-median baseline, and the bulk of the MAE drop happens through the middle and upper third. The poor performance at layer 0 (the token-embedding output) is itself informative: if the probe were reading off surface features of the current token, the token identity or its embedding, the embedding-layer probe would already match the headline numbers. The signal the probe recovers is therefore a processed representation that emerges only after several layers of computation, not a property of the current token in isolation.

Second, the all-layers probe used for the headline numbers in §4 (where h_t is the concatenation of the hidden state at every layer) significantly outperforms every single-layer probe in Figure 4 — the corresponding all-layers cell of Table 2 is well below the best single-layer entry — indicating that no single layer is sufficient and that information from multiple layers contributes additively to the linear readout.

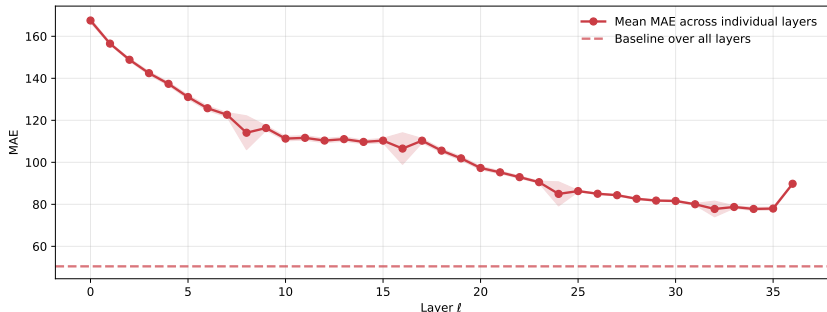


Figure 4: Per-layer probe MAE. MAE-vs-layer for the Remaining Count Probe. Layer 0 = embedding output; layer L = final hidden state. The dashed horizontal line marks the constant-median statistical baseline.

A.2 MAE relative to the statistical-baseline floor

The absolute MAE numbers in Tables 1 and 2 are reported in tokens, which makes within-row comparisons easy but cross-dataset comparisons harder: a MAE = 30 on a dataset whose constant-median baseline is 50 is a different result from the same number on a dataset whose constant-median baseline is 200. Tables 4 and 5 re-report the same numbers, each entry divided by the corresponding constant-median statistical-baseline MAE (the MAD-about-the-median floor of §3.4). On this scale, values below 1 mean the probe beats the constant baseline and values above 1 mean it loses; the constant-baseline row of Table 2 is omitted because it is identically 1.00 by construction.

Read in this normalized form, the natural-language datasets cluster in the 0.5–0.9 range (the probe extracts roughly 10–50% of the floor’s gap to zero), the synthetic Count and Countdown sets in the 0.04–0.7 range (probe extracts most of the floor), and the one notable null result — Llama-3.1-8B / TriviaQA — is now obvious: the Exact countdown predictor is identically tied with the constant baseline (1.00), and the Remaining Count Probe extracts only an 0.18 improvement, the smallest natural-language gain in the table.

A.3 MAE by completion length

The headline numbers in Tables 1 and 2 are token-weighted averages over the eval split. Figure 5 shows the per-completion-length breakdown of the Remaining Count Probe MAE on the eval split

Table 4: Relative version of Table 1: prompt-end AE of the Completion Length Probe divided by the corresponding constant-median statistical-baseline AE. Smaller is better; values below 1 mean the probe beats the constant baseline. Mistral-7B / TriviaQA omitted (“-”); see §3.7.

Model	Count	Countdown	GSM8K	MATH	MMLU-Pro	OpenThoughts-1k	TriviaQA
Llama-3.1-8B	0.20	0.04	0.72	0.69	0.57	0.67	0.76
Olmo-3-7B	0.21	0.06	0.69	0.68	0.66	0.73	0.69
Mistral-7B	0.51	0.14	0.88	0.76	0.67	0.84	-

Table 5: Relative version of Table 2: per-token MAE divided by the constant-median statistical-baseline MAE. The Statistical-baseline row of Table 2 is omitted from this version because it is identically 1.00 by construction. Smaller is better; values below 1 mean the predictor beats the constant baseline, values at or above 1 mean it ties or loses. Mistral-7B / TriviaQA omitted (“-”); see §3.7.

Model	Count	Countdown	GSM8K	MATH	MMLU-Pro	OpenThoughts-1k	TriviaQA
Llama-3.1-8B							
Exact countdown	0.25	0.04	0.63	0.82	0.71	0.69	1.00
Remaining Count Probe	0.29	0.04	0.52	0.73	0.72	0.70	0.82
Olmo-3-7B							
Exact countdown	0.27	0.07	0.76	0.74	0.69	0.88	0.93
Remaining Count Probe	0.29	0.04	0.62	0.69	0.72	0.89	0.77
Mistral-7B							
Exact countdown	0.70	0.19	0.90	0.82	0.82	0.88	-
Remaining Count Probe	0.35	0.10	0.73	0.76	0.81	0.74	-

on Llama-3.1-8B / GSM8K. Three things are worth noting. First, MAE is lowest for completions whose total length sits near the dataset mode (the 130–220-token range, MAE \approx 20–30), where most of the training mass lives. Second, the short- T tail (80–110 tokens) is mildly worse (MAE \approx 40–50) and has few samples per bin, so the estimate is noisier. Third, the long- T tail ($T > 300$) degrades sharply: bins in the 400–460 range have MAE in the 80–130 range. This is the regime from which the curated retraction examples in §4.3 are drawn: the absolute-error caveat in that section — “the probe reads 4.84 against a true $r_t = 814$ ” — is consistent with the bin-wise picture rather than being an outlier of one completion. On completions whose total length falls in the worst bins of this figure, the probe’s absolute predictions are systematically far from r_t .

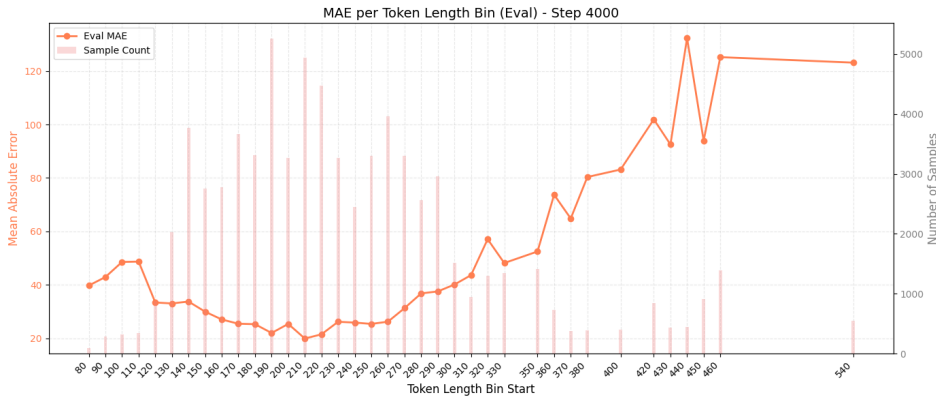


Figure 5: Per-token-length-bin MAE of the Remaining Count Probe on the eval split, at end of training (step 4000) on Llama-3.1-8B / GSM8K. Bin width 10 tokens. Orange line and left axis: bin-mean MAE in tokens. Coral bars and right axis: number of eval-split samples per bin. Probe accuracy is best on completions whose total length sits near the dataset mode (130–220 tokens, MAE \approx 20–30) and degrades for very long completion, which are much less frequent in the training dataset; the long- T tail ($T > 300$) is where the curated retraction examples of §4.3 live and where the probe’s absolute predictions are systematically far from r_t .

A.4 Training hyperparameters and dataset sizes

Table 6 lists the probe-training hyperparameters used to produce every number in §4 and the appendix; Table 7 lists the configured train and eval split sizes per dataset. The base model is held frozen under `torch.no_grad()` throughout; only the per-probe linear heads are trained. Each head has its own AdamW optimizer stepped on its own loss for every minibatch (§3, “Loss and Optimization”). All configurations are reproducible from the released repository (<https://anonymous.4open.science/r/llm-output-length>); the per-run `config.yaml` snapshot in each output directory records the exact values used.

Table 6: Probe-training hyperparameters. Defaults from the released code.

Setting	Value	Notes
Optimizer (per probe head)	AdamW	one optimizer per active probe head
Learning rate	2×10^{-4}	shared across probe heads
Weight decay	0.01	
Max gradient norm	10.0	gradient clipping
Loss (regression)	MSE	for <code>count</code> , <code>percentage</code> , <code>prompt_only_count</code>
Loss (classification)	soft cross-entropy	with anchor sigma 0.15 (§A.8)
LR scheduler	ReduceLRonPlateau	monitor <code>eval_mae</code> , factor 0.5, patience 5 eval steps, min LR = 10^{-7}
Max steps	4000	
Batch size (per device)	8	training and eval; same across probes
Gradient accumulation	1	
Eval cadence	every 100 steps	ReduceLRonPlateau consumes <code>eval_mae</code> from these evals
Probe input layer	all layers concatenated	<code>data.hidden_layer = "all"</code>
Independent seeds	{0, 1, 2}	seeds threaded through Torch / NumPy / Python / HF Trainer / dataloader
Hidden-state extraction	frozen forward pass	<code>torch.no_grad()</code> over the full (prompt, completion) sequence
Generation (extraction)	<code>max_new_tokens = 1024</code>	<code>do_sample=True</code> , $T = 0.7$, $top-p = 0.8$, $top-k = 20$
Naturally-terminated filter	<code>has_eos = True</code> only	sequences that hit <code>max_new_tokens</code> excluded (§3)

Table 7: Configured train / eval split sizes per dataset, as set in `src/miol/conf/data/`. The actual number of samples used by each probe is at most the configured size minus those whose generation hit the `max_new_tokens` cutoff (filtered by `has_eos`; see §3.7); per-(model, dataset) effective counts vary slightly with the model’s termination behavior.

Dataset	Train	Eval	Source / split convention
Count	301	301	synthetic, $n \in \{0, \dots, 300\}$, one completion per length
Countdown	301	301	synthetic, $n \in \{0, \dots, 300\}$, one completion per length
GSM8K	7,473	1,319	full <code>train / test</code> splits
MATH	$\approx 7,500$	$\approx 5,000$	concatenation of seven subject configs
MMLU-Pro	10,000	2,256	first 10,000 for train, last 2,256 for eval
OpenThoughts-1k	800	200	first 800 / last 200 of the 1k sample
TriviaQA	10,000	2,000	first 10,000 for train, last 2,000 for eval

A.5 Prompt templates

For every dataset, the input to the base model is a chat-template-formatted message consisting of a fixed system prompt and a user message. We do not preprocess or rephrase prompts beyond formatting them with each model’s chat template. Table 8 reproduces the system prompt for every dataset used in the paper and lists where the user-message body comes from — a synthetic template (already given verbatim in §3.7) for Count and Countdown, and a HuggingFace dataset column for the natural-language sets. The exact configuration is preserved in `src/miol/conf/data/` in the released repository (<https://anonymous.4open.science/r/llm-output-length>).

A.6 Cross-dataset generalization on Mistral-7B-Instruct-v0.3

A.7 Cross-dataset generalization on Olmo-3-7B-Instruct

A.8 Classification probe family — full breakdown

Alongside the three regression predictors of §3.3, we train a complementary family of K -way classifiers ($K \in \{2, 3, 5, 7, 9\}$) on $h_i^{(\ell)}$, with anchors $a_i = i/(K - 1)$ for $i = 0, \dots, K - 1$ over

Table 8: System prompts and user-message source for each dataset. The synthetic user-message templates for Count and Countdown are reproduced verbatim in §3.7; for the natural-language datasets the user message is the indicated HuggingFace column for the example, used unmodified.

Dataset	System prompt	User message source
Count	“You are a helpful assistant that follows instructions precisely. When asked to generate tokens, you produce exactly the requested number of tokens.”	template (§3.7)
Countdown	“You are a helpful assistant that follows instructions precisely. When asked to generate tokens, you produce exactly the requested number of tokens.”	template (§3.7)
GSM8K	“You are a helpful math tutor that solves grade school math problems step by step.”	question field
MATH	“You are a helpful math tutor that solves math problems step by step.”	problem field
MMLU-Pro	“You are a helpful assistant that solves problems step by step.”	question field
OpenThoughts-1k	“You are a helpful assistant that solves problems step by step.”	problem field
TriviaQA	“You are a helpful assistant that solves problems step by step.”	question field

Table 9: Remaining Count Probe cross-token MAE (mean across 3 seeds) on Mistral-7B. Each train-dataset row is followed by a *baseline* row giving the median-baseline MAE fit on that dataset’s train split. Reported on the five datasets for which the full train×eval grid was available; MATH and TriviaQA are omitted from this matrix, see §3.7. The Olmo-3-7B counterpart (Table 10) reports all seven.

Train	Count	Countdown	GSM8K	MMLU-Pro	OpenThoughts-1k
Count	71.75	188.31	120.75	229.31	262.99
<i>baseline</i>	197.45	200.48	147.94	170.32	179.64
Countdown	257.66	21.09	124.40	208.53	226.64
<i>baseline</i>	197.77	200.23	158.71	172.72	179.93
GSM8K	247.25	277.57	60.93	142.28	170.10
<i>baseline</i>	228.80	236.82	91.67	187.53	215.33
OpenThoughts-1k	181.93	219.30	139.60	128.60	132.99
<i>baseline</i>	197.54	200.27	153.61	171.51	179.71

Table 10: Remaining Count Probe cross-token MAE (mean across 3 seeds) on Olmo-3-7B. Each train-dataset row is followed by a *baseline* row giving the median-baseline MAE fit on that dataset’s train split.

Train	Count	Countdown	GSM8K	MATH	MMLU-Pro	OpenThoughts-1k	TriviaQA
Count	28.97	119.08	169.72	258.82	271.78	310.52	185.82
<i>baseline</i>	116.54	117.84	124.24	192.66	202.63	242.21	150.64
Countdown	169.18	4.57	185.80	284.90	292.47	339.74	191.86
<i>baseline</i>	116.55	117.84	124.30	192.35	202.28	241.83	150.71
GSM8K	103.51	115.47	80.95	147.89	174.40	203.76	135.60
<i>baseline</i>	117.37	118.86	124.32	199.78	210.38	250.50	150.13
MMLU-Pro	125.74	108.26	130.51	133.27	134.73	174.52	158.45
<i>baseline</i>	149.74	149.57	165.18	180.69	184.82	218.29	184.97
OpenThoughts-1k	106.65	104.97	129.57	130.81	150.49	178.03	150.73
<i>baseline</i>	141.65	141.71	156.11	179.30	184.35	219.01	177.60
TriviaQA	110.91	124.37	102.90	174.14	164.93	220.76	117.25
<i>baseline</i>	119.47	121.09	126.04	206.57	217.60	258.09	151.00

the normalized completion progress $u_t = t/(T - 1)$. At $K = 2$ the classifier predicts whether the current token is in the first or the second half of the output; at $K = 9$ it predicts which ninth. The chance-corrected scale of Cohen’s κ lets us compare across K : a non-trivial κ at $K = 9$ indicates the residual stream encodes a finer-grained progress signal than a coarse early/late split. Table 11 reports κ across all (model, dataset) cells.

The pattern is consistent across models: κ degrades smoothly with K and is highest on the synthetic sets, where completion length is fully determined by the prompt, and lowest on TriviaQA, consistent with its short and variable answer lengths.

Table 11: Full per-(model, dataset) dataset-wide Cohen’s κ for the classification probe family $K \in \{2, 3, 5, 7, 9\}$.

K	2	3	5	7	9
Llama-3.1-8B					
Count	0.966	0.942	0.912	0.819	0.774
Countdown	0.983	0.990	0.935	0.911	0.775
GSM8K	0.838	0.804	0.693	0.553	0.463
MATH	0.744	0.707	0.559	0.427	0.332
MMLU-Pro	0.744	0.677	0.516	0.385	0.300
OpenThoughts-1k	0.766	0.697	0.545	0.420	0.332
TriviaQA	0.617	0.549	0.380	0.280	0.222
Olmo-3-7B					
Count	0.949	0.919	0.878	0.809	0.708
Countdown	0.976	0.985	0.926	0.900	0.903
GSM8K	0.823	0.769	0.646	0.519	0.422
MATH	0.777	0.714	0.574	0.447	0.358
MMLU-Pro	0.770	0.709	0.554	0.412	0.330
OpenThoughts-1k	0.707	0.547	0.380	0.272	0.208
TriviaQA	0.705	0.636	0.439	0.324	0.250
Mistral-7B					
Count	0.951	0.919	0.863	0.786	0.672
Countdown	0.990	0.976	0.946	0.927	0.863
GSM8K	0.793	0.762	0.625	0.506	0.414
MATH	0.723	0.697	0.548	0.407	0.315
MMLU-Pro	0.754	0.704	0.540	0.416	0.332
OpenThoughts-1k	0.732	0.679	0.524	0.379	0.315

A.9 Additional examples of retraction and count spiking

Selection procedure. The four panels below were obtained by sorting eval-set completions on per-completion MAE and walking down from the worst; they are by construction drawn from the high-loss region of the eval set, not a random sample. On these completions the probe’s *absolute* predictions are far from the ground truth, so the figures are licensed to support a directional, qualitative claim only: that the probe’s per-position prediction *moves upward* at the retraction token, not a claim about absolute remaining-count accuracy. The dynamic re-estimation phenomenon documented in §4.3 is illustrated there on a single curated retraction example (Figure 3); the Limitations section notes that a systematic analysis, pairing retraction-token shifts with a length-matched non-retraction control population and reporting the aggregate distribution of upward shifts in \hat{r}_t , is the strongest version of this result and remains future work. As partial qualitative support in advance of that aggregate study, we collect below four additional examples from the same high-loss selection procedure. The pattern that recurs in those high-loss completions is precisely a retraction-token shift: the ground-truth r_t continues to decrement monotonically while the probe’s \hat{r}_t jumps upward, so the contribution to MAE around the retraction is large by construction. Each panel was captured from an interactive token-by-token explorer that displays, for every completion position t , the underlying token, the ground-truth remaining count r_t , and the Remaining Count Probe’s per-position prediction \hat{r}_t (count pred column in the table at the top of each panel and bar height in the chart at the bottom).

The takeaway in every panel is qualitatively the same as in §4.3: at a token where the model concedes that its current line of work is wrong — “Wait”, “But”, “contradiction”, “let’s check”, “let’s look again” — \hat{r}_t jumps sharply upward, while the true remaining count r_t continues to decrement monotonically. The four examples below show the spike triggered by different retraction phrases at different absolute positions in the completion, suggesting the pattern is not tied to a single trigger token.

We make no quantitative claim about the prevalence of the pattern from a four-example gallery; the systematic version is flagged as future work in Limitations.

457	"he"	COMPL	498	0.521	194.669	303.348	317.744	66.91%	63.22%	87.59%	92.58%	-2.648
458	"had"	COMPL	497	0.520	190.382	297.698	315.864	59.99%	62.82%	85.51%	91.73%	-2.726
459	"taken"	COMPL	496	0.519	206.876	299.124	309.839	58.29%	61.74%	82.27%	89.40%	-2.508
460	"***"	COMPL	495	0.518	179.389	315.420	307.932	63.76%	61.64%	93.69%	89.20%	-1.967
461	"B"	COMPL	494	0.517	136.845	357.955	318.287	72.46%	62.25%	113.63%	96.63%	-6.522
462	","	COMPL	493	0.516	167.287	325.793	312.892	66.68%	62.90%	98.69%	92.91%	-1.474
463	"g"	COMPL	492	0.515	212.224	279.276	316.997	56.87%	62.64%	79.46%	91.40%	-2.035
464	"g"	COMPL	491	0.514	243.499	247.518	393.470	58.41%	61.24%	67.48%	88.72%	-6.769
465	"g"	COMPL	490	0.513	171.491	318.589	386.170	65.89%	63.21%	96.30%	89.21%	-2.126
466	"steps"	COMPL	489	0.512	228.205	268.795	308.412	54.97%	66.87%	75.89%	88.62%	-3.492
467	"***"	COMPL	488	0.511	192.948	295.852	290.583	66.46%	66.82%	86.66%	87.93%	-3.366
468	".\n\n"	COMPL	487	0.510	244.316	242.084	294.882	49.83%	59.81%	66.37%	86.02%	-1.507
469	"Wait"	COMPL	486	0.509	352.843	133.157	278.485	27.49%	56.72%	31.75%	80.97%	-6.994
470	"--"	COMPL	485	0.508	330.584	145.496	261.473	38.60%	53.35%	35.29%	75.13%	-1.891
471	"that"	COMPL	484	0.507	296.796	185.294	244.287	38.29%	49.93%	47.35%	68.51%	-1.135
472	"**"	COMPL	483	0.506	319.392	163.688	227.988	33.87%	46.71%	48.70%	62.72%	-3.651
473	"a"	COMPL	482	0.505	317.287	164.713	216.482	34.17%	44.44%	41.21%	58.89%	-6.083
474	"contradiction"	COMPL	481	0.504	298.907	182.893	289.940	37.86%	43.18%	46.79%	56.82%	-2.811
475	".\n\n"	COMPL	480	0.503	325.856	154.144	193.583	32.11%	39.90%	38.26%	51.02%	-2.241
476	"Wait"	COMPL	479	0.503	314.284	164.716	183.806	34.30%	37.84%	41.63%	47.50%	-1.817

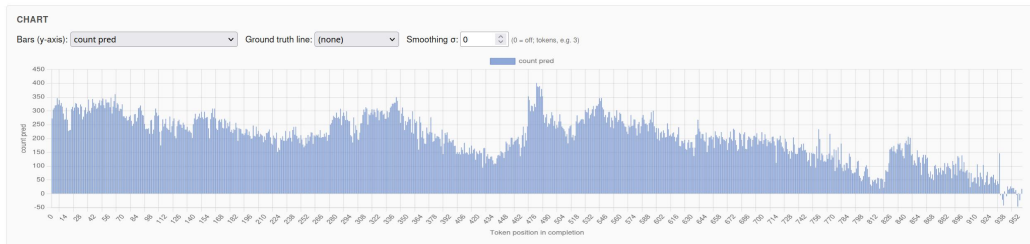


Figure 6: Retraction example 1. Around completion position 469 the model emits “Wait -- that’s a contradiction” after writing out a multi-step arithmetic answer. The count pred column shows \hat{r}_t jumping to ≈ 353 at the "Wait" token (row 469) and remaining elevated through the retraction phrase, while the true r_t continues to decrement monotonically.

598	"4"	COMPL	407	0.496	174.862	232.138	219.554	57.64%	53.37%	79.79%	72.97%	-6.984
597	"-"	COMPL	406	0.495	173.625	232.975	219.572	57.38%	53.51%	80.47%	73.25%	-6.793
596	"--"	COMPL	405	0.494	233.456	171.544	215.242	42.36%	52.57%	53.74%	71.64%	-6.866
599	"1"	COMPL	404	0.493	154.831	249.169	228.756	61.68%	54.85%	89.18%	74.43%	-6.986
600	"6"	COMPL	403	0.492	218.068	184.932	228.882	45.89%	53.98%	59.55%	74.21%	-6.409
601	"**"	COMPL	402	0.491	174.393	227.687	228.288	56.62%	54.16%	78.88%	74.67%	-6.568
602	"***"	COMPL	401	0.490	171.659	229.358	219.881	57.19%	54.83%	80.18%	74.41%	-6.612
603	"2"	COMPL	400	0.399	166.643	233.357	228.856	58.34%	54.60%	82.30%	75.51%	-1.465
604	"6"	COMPL	399	0.398	206.962	192.998	218.274	48.36%	54.09%	63.77%	74.58%	-4.527
605	"flash"	COMPL	398	0.397	153.885	244.115	219.813	61.24%	54.62%	88.47%	75.64%	-1.836
606	"lights"	COMPL	397	0.396	223.172	173.828	213.982	43.79%	53.29%	56.86%	73.27%	-2.922
607	"**\n\n"	COMPL	396	0.395	257.128	138.872	284.571	35.07%	53.06%	42.53%	69.47%	-6.097
608	"Wait"	COMPL	395	0.394	368.757	26.243	198.841	6.64%	47.49%	6.87%	64.79%	-6.310
609	"--"	COMPL	394	0.393	345.135	48.865	179.811	12.40%	42.56%	13.22%	57.19%	-2.064
610	"but"	COMPL	393	0.392	319.999	73.001	158.818	18.58%	39.83%	20.48%	53.28%	-3.147
611	"that"	COMPL	392	0.391	327.855	64.346	142.491	16.41%	35.81%	17.88%	47.17%	-1.734
612	"would"	COMPL	391	0.390	267.673	123.217	131.809	31.54%	32.25%	37.45%	42.81%	-2.188
613	"mean"	COMPL	390	0.389	252.585	137.415	122.295	35.23%	38.94%	42.77%	38.95%	-3.660
614	"each"	COMPL	389	0.388	224.205	164.795	119.481	42.36%	38.34%	53.75%	37.95%	-1.741
615	"person"	COMPL	388	0.387	267.032	120.968	107.166	31.18%	27.32%	36.93%	32.79%	-2.854
616	"has"	COMPL	387	0.386	268.194	118.886	101.664	38.70%	26.01%	36.27%	30.81%	-1.138
617	"one"	COMPL	386	0.385	228.485	157.515	103.528	40.81%	26.59%	51.27%	31.69%	-6.312

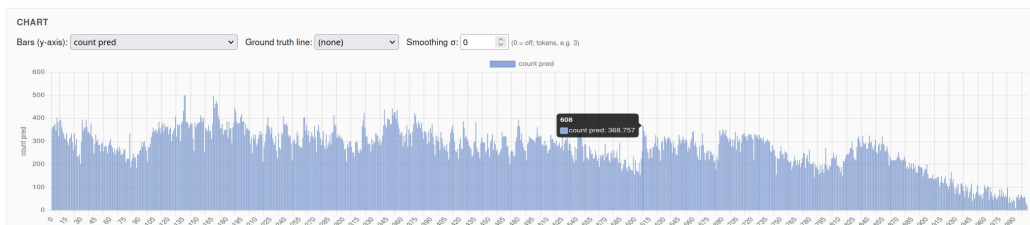


Figure 7: Retraction example 2. Around completion position 608, after the model has written a candidate answer “**20 flashlights**”, it follows with “Wait -- but that would mean . . .” and the bar chart shows a corresponding upward excursion. The "Wait" token at row 608 has $\hat{r}_t \approx 369$ (tooltip), against the surrounding ≈ 130 – 170 range.

254	"lt"	COMPL	599	0.792	235.226	363.774	345.966	69.73%	57.33%	87.21%	80.53%	-1.476
255	"t"	COMPL	598	0.791	244.996	353.884	344.988	59.83%	57.27%	83.75%	80.40%	-2.322
256	"more"	COMPL	597	0.789	269.874	327.926	341.671	54.93%	56.81%	75.73%	79.51%	-1.967
257	"than"	COMPL	596	0.699	234.417	361.583	345.515	68.67%	57.55%	87.08%	80.94%	-2.438
258	" "	COMPL	595	0.698	229.189	365.828	351.785	61.49%	58.69%	88.77%	83.13%	-8.875
259	"4"	COMPL	594	0.696	255.855	338.145	352.277	58.39%	58.86%	79.58%	83.37%	-1.225
260	"hours"	COMPL	593	0.695	255.812	337.188	352.429	56.89%	58.98%	79.45%	83.71%	-1.232
261	".\n\n"	COMPL	592	0.694	366.047	225.953	339.415	38.17%	56.88%	47.17%	80.62%	1.338
262	"But"	COMPL	591	0.693	382.892	208.188	323.789	35.21%	54.34%	42.74%	75.60%	-6.607
263	"let"	COMPL	590	0.692	349.751	240.249	312.175	48.72%	52.47%	51.13%	72.26%	1.507
264	"s"	COMPL	589	0.691	354.712	234.288	299.226	39.78%	56.38%	49.65%	68.58%	0.927
265	"check"	COMPL	588	0.689	368.329	219.671	285.893	37.36%	48.21%	45.94%	64.72%	-1.725
266	"she"	COMPL	587	0.688	388.796	278.284	286.921	47.39%	47.46%	62.11%	63.38%	-8.262
267	"exact"	COMPL	586	0.687	386.564	279.436	272.766	47.69%	46.16%	62.61%	60.62%	-8.178
268	"wording"	COMPL	585	0.686	320.147	264.853	262.610	45.27%	44.54%	58.52%	57.89%	-8.336
269	".\n\n"	COMPL	584	0.685	292.139	291.861	257.981	49.98%	43.84%	66.62%	56.60%	0.499
270	"s"	COMPL	583	0.683	284.152	298.848	254.147	51.26%	43.28%	68.93%	55.54%	-8.888
271	"s"	COMPL	582	0.682	275.498	306.582	262.282	52.66%	44.73%	71.49%	57.97%	-2.884
272	"p"	COMPL	581	0.681	249.519	331.481	274.539	57.85%	46.92%	79.62%	61.68%	-1.652
273	"isn"	COMPL	580	0.680	241.142	337.858	286.388	58.25%	48.67%	82.19%	64.79%	-2.513
274	"s"	COMPL	579	0.679	253.564	325.436	293.415	56.21%	56.31%	78.18%	67.64%	-1.287
275	"work"	COMPL	578	0.678	243.372	334.628	304.911	57.89%	52.37%	81.48%	71.20%	-2.318

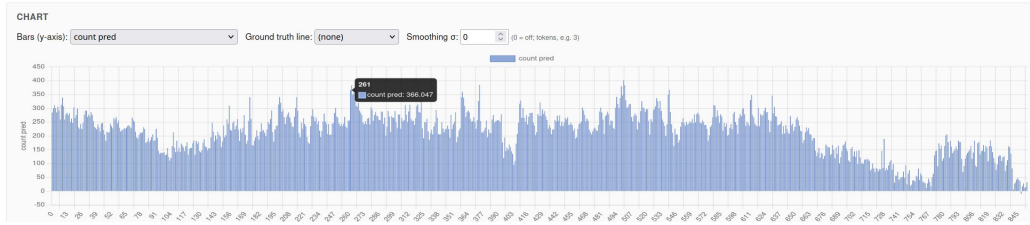


Figure 8: Retraction example 3. Around completion position 261 the model writes “. \n\n But let’s check the exact wording” immediately after producing a candidate numerical answer. The count pred column climbs from the surrounding ≈ 220 – 280 range to a local peak of $\hat{r}_t \approx 366$ at the start of the reconsideration and stays elevated for the next several tokens.

493	".\n\n"	COMPL	360	0.422	382.848	57.152	182.383	15.88%	28.10%	17.24%	33.03%	0.468
494	"But"	COMPL	359	0.421	341.497	17.583	94.368	4.88%	25.94%	5.89%	30.48%	-8.715
495	"let"	COMPL	358	0.420	316.259	41.741	89.367	11.66%	24.61%	12.38%	28.67%	0.934
496	"s"	COMPL	357	0.419	361.189	55.888	87.899	15.64%	24.01%	16.97%	28.14%	0.301
497	"look"	COMPL	356	0.417	336.988	19.012	89.186	6.34%	22.16%	5.49%	25.88%	-2.343
498	"again"	COMPL	355	0.416	379.895	24.895	76.807	7.81%	19.42%	6.78%	22.58%	-3.829
499	".\n\n"	COMPL	354	0.415	347.564	6.436	59.911	1.82%	16.63%	1.83%	19.19%	-8.607
500	"Wait"	COMPL	353	0.414	401.594	48.594	53.959	13.77%	15.02%	12.88%	16.97%	-8.515
501	" "	COMPL	352	0.413	384.316	32.316	43.857	9.18%	12.26%	8.78%	13.34%	-1.671
502	"perhaps"	COMPL	351	0.411	329.665	21.335	32.482	6.80%	9.12%	6.27%	9.36%	-1.283
503	"she"	COMPL	350	0.410	361.862	48.138	31.581	13.75%	8.81%	14.77%	9.11%	-8.432
504	"phrase"	COMPL	349	0.409	396.585	42.415	34.872	12.15%	9.64%	12.94%	9.91%	-8.621
505	"is"	COMPL	348	0.408	316.119	31.881	33.886	9.16%	9.39%	9.69%	9.63%	-1.426
506	"s"	COMPL	347	0.407	315.531	31.469	30.649	9.07%	8.73%	9.59%	8.88%	-1.591
507	".\n\n"	COMPL	346	0.406	268.621	77.379	36.486	22.36%	16.44%	25.18%	10.85%	-3.174
508	"she"	COMPL	345	0.404	252.798	92.282	43.216	26.73%	12.41%	30.85%	13.26%	-2.883
509	"look"	COMPL	344	0.403	272.618	71.382	49.711	28.75%	14.30%	23.15%	15.39%	-4.694
510	"well"	COMPL	343	0.402	261.858	61.862	51.848	18.86%	14.75%	19.86%	16.89%	-2.398
511	"over"	COMPL	342	0.401	274.321	67.679	54.584	19.79%	15.79%	21.96%	17.41%	-2.609
512	" "	COMPL	341	0.400	224.138	116.878	64.138	34.27%	18.61%	41.36%	20.92%	-8.858
513	"4"	COMPL	340	0.399	253.426	86.574	67.981	25.46%	19.78%	29.18%	22.26%	-2.214
514	"hours"	COMPL	339	0.397	247.312	91.688	72.988	27.85%	21.27%	31.28%	24.19%	-2.877

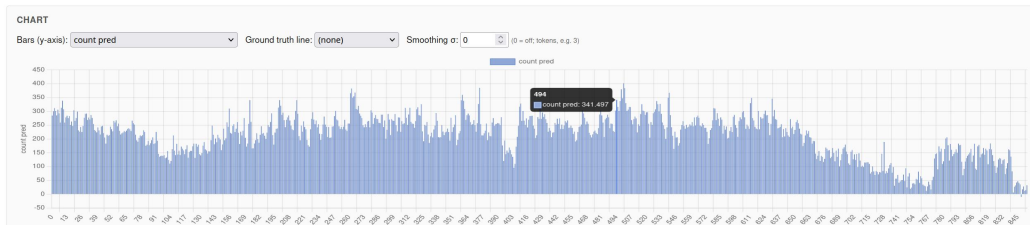


Figure 9: Retraction example 4. Around completion position 500 the model produces a doubled retraction: “But let’s look again. \n\n Wait -- perhaps the phrase ...”. The count pred column spikes to $\hat{r}_t \approx 341$ at the "But" token (row 494) and shows a second elevated cluster around the subsequent "Wait".